Journal of Biogeography (J. Biogeogr.) (2016) 43, 2099–2112

ORIGINAL ARTICLE

A zoogeographical boundary between the Palaearctic and Sino-Japanese realms documented by consistent north/south phylogeographical divergences in three woodland birds in eastern China

Gang Song[1,2†], Ruiying Zhang[1,3†], Yanhua Qu[1], Zhiheng Wang[4,5], Lu Dong[6], Anton Kristin[7], Per Alström[1,8,9], Per G. P. Ericson[10], David M. Lambert[2], Jon Fjeldså[5] and Fumin Lei[1*]

[1]Key Laboratory of Zoological Systematics and Evolution, Institute of Zoology, Chinese Academy of Sciences, Beijing 100101, China, [2]Environmental Futures Research Institute, Griffith University, Nathan, QLD 4111, Australia, [3]Center for Developmental Biology, Institute of Genetics and Developmental Biology, Chinese Academy of Sciences, Beijing 100101, China, [4]Department of Ecology and Key Laboratory for Earth Surface Processes of the Ministry of Education, College of Urban and Environmental Sciences, Peking University, Beijing 100871, China, [5]Center for Macroecology, Evolution and Climate at the Natural History Museum of Denmark, University of Copenhagen, Copenhagen, Denmark, [6]Ministry of Education Key Laboratory for Biodiversity and Ecological Engineering, College of Life Sciences, Beijing Normal University, Beijing 100875, China, [7]Institute of Forest Ecology SAS, 96053 Zvolen, Slovakia, [8]Swedish Species Information Centre, Swedish University of Agricultural Sciences, PO Box 7007, SE-75007 Uppsala, Sweden, [9]Department of Animal Ecology, Evolutionary Biology Centre, Uppsala University, Norbyvägen 18D, 752 36 Uppsala, Sweden, [10]Swedish Museum of Natural History, PO Box 50007, SE-10405 Stockholm, Sweden

*Correspondence: Fumin Lei, Key Laboratory of Zoological Systematics and Evolution, Institute of Zoology, Chinese Academy of Sciences, Beijing 100101, China.
E-mail: leifm@ioz.ac.cn
†These authors contributed equally to this work.

ABSTRACT

Aim The location of zoogeographical boundaries in eastern China has long been the subject of debate. To identify any north/south genetic divergence between the Palaearctic and Sino-Japanese realms proposed by previous studies, we conducted a comparative phylogeographical study involving three passerine species with wide latitudinal distributions in eastern China.

Location Eastern China.

Methods Two mitochondrial genes and three nuclear introns were amplified and sequenced. Population structures were analysed using intra-specific phylogeny, TCS networks, AMOVA and structure inferences. We tested for evidence of genetic barriers based on pairwise differences. Lineage divergences, demographic dynamics and gene flow between lineages were estimated using Bayesian methods.

Results A congruent north/south phylogeographical divergence was identified for three species. A geographical barrier was inferred at *c.* 40° N in eastern China. The population sizes of the northern and southern lineages have both been stable through the late Pleistocene, while multiple divergences were inferred during the early and middle Pleistocene.

Main conclusions Our results suggest a general phylogeographical break in north-eastern China, coinciding with the Palaearctic/Sino-Japanese boundary. Physical blocking of the Yan Mountains and fragmentation of suitable habitat during glacial stages between the north and south probably acted together to provide long-lasting barrier effects. Our comparative phylogeographical approach demonstrates that the Palaearctic/Sino-Japanese boundary may represent a gene-flow barrier even within widespread species.

Keywords
Aegithalos caudatus*, comparative phylogeography, early Pleistocene, eastern Asia, lineage divergence, *Poecile montanus*, *Poecile palustris

INTRODUCTION

In 'The Geographical Distribution of Animals', Alfred Russel Wallace intuitively classified the fauna of eastern China as representative of the Palaearctic region, bordering on the Oriental region in the south (Wallace, 1876). However, he also noted that a subregion within the Palaearctic realm, Japan and northern China, stood out as 'an interesting and very productive district' while commenting '... Its limits are not very well defined' (Wallace, 1876). Recently,

© 2016 John Wiley & Sons Ltd

doi:10.1111/jbi.12758

Procheş & Ramdhani (2012) noted similarities between the eastern China and Himalayan regions and identified them as a distinct faunistic cluster of the Sino-Himalayan subregion. In a recent large-scale biogeographical analysis, Holt *et al.* (2013) identified a distinct Sino-Japanese realm extending from Tibet in the west to the major Japanese archipelago in the east. However, the basis for recognizing this area as a separate realm was questioned by other biogeographers (e.g. Kreft & Jetz, 2013), who instead considered this as a transition zone between the Palaearctic and Oriental realms.

Traditional zoogeographical classification places the boundary between the Oriental and Palaearctic realms at the Qinling Mountains – Huai River, around 32°–34° N in eastern China (Cheng, 1987; Zhang, 1999; Tan, 2011). The results obtained by Holt *et al.* (2013) suggested the existence of some old endemic groups and a sharp boundary between the old fauna of the Oriental lowland monsoon forests and more derived and species-rich clades containing babblers, leaf warblers, tits, etc. The latter primarily radiated in the colder and semi-deciduous environments of the Sino-Himalayan mountains. However, as a consequence of climatic instability since the late Miocene, China's montane environments have also received a strong influx of groups that may have originated in the vast forest and woodland regions in the eastern Palaearctic (Päckert *et al.*, 2012). According to Holt *et al.* (2013), in eastern China, the Palaearctic/Sino-Japanese boundary is located at *c.* 40°–41° N. This is in agreement with other quantitative evidence (Kreft & Jetz, 2010; Procheş & Ramdhani, 2012) but is more northwards than the traditional Palaearctic/Oriental boundary (Fig. 1).

To understand the nature of a biogeographical break, it may also be relevant to examine the phylogeographical structure of the species that are distributed across the break. Phylogeographical studies mostly focus on the evolutionary processes that have operated over more recent time scales than those typically considered in deep-time biogeographical analyses (Avise, 1992; Burton, 1998; Arbogast & Kenagy, 2001; Eberl *et al.*, 2013). With this change in focus, we may establish whether the boundary is underpinned by selection filters or by continued breaks in gene flow among populations. A long-lasting geographical filter can be documented by multiple divergent events that have occurred at different times in the same geographical region (Lei *et al.*, 2015). Therefore, a closer examination of phylogeographical patterns in more organisms is needed to assess whether historical or environmental factors related to the Palaearctic/Sino-Japanese boundary have caused a divergence between northern and southern populations in eastern China.

A phylogeographical break between populations living north and south of the Palaearctic/Sino-Japanese boundary has been recorded in some organisms (Zhang *et al.*, 2008; Bai *et al.*, 2010; Sakka *et al.*, 2010; Ding *et al.*, 2011). Studies on some generalist birds such as the great tit, *Parus major*; the common pheasant, *Phasianus colchicus*; and the Eurasian magpie, *Pica pica*, which tolerate a broad range of ecological conditions, did not reveal any major divergence among populations of the north and south (Liu *et al.*, 2010; Zhang *et al.*, 2012; Zhao *et al.*, 2012). In contrast, the azure-winged magpie, *Cyanopica cyanus*, which is more dependent on a well-wooded habitat, showed a north/south genetic division in eastern China (Zhang *et al.*, 2012). We hypothesize that phylogeographical breaks among populations in the northern and southern parts of eastern China might be recorded in other avian species as well, especially in sedentary woodland species.

In this study, we focused on three woodland birds with large latitudinal distributions in northern Eurasia: the marsh tit, *Poecile palustris* Linnaeus, 1758; the willow tit, *Poecile montanus* Conrad, 1827; and the long-tailed tit, *Aegithalos caudatus* Linnaeus, 1758. These species are small-sized passerines that are widely distributed across the northern temperate belt from the Atlantic to the Pacific coasts. The three species are found in lowland, submontane and montane mature deciduous woodlands and forests with well-developed shrub layers. The distributional ranges of all three species cover major areas of eastern China and extend across the boundary between the Palaearctic and Sino-Japanese Realms (Gosler & Clement, 2007; Harrap, 2008).

Mitochondrial and nuclear markers revealed that *A. caudatus* is divided into a widespread northern clade and an eastern Chinese clade (Päckert *et al.*, 2010; Song *et al.*, 2015). These are sometimes treated as separate species, *A. caudatus sensu stricto* and *A. glaucogularis* (e.g. Harrap, 2008; Gill & Donsker, 2015). With respect to *P. montanus*, analyses of mitochondrial DNA from western Europe to eastern Russia and Japan failed to detect any phylogeographical structure (Kvist *et al.*, 2001; Salzburger *et al.*, 2002; Zink *et al.*, 2008). However, the geographically isolated subspecies *P. m. songarus* (central Asia), *P. m. affinis* (north-central China) and *P. m. weigoldicus* (south-central China) were genetically divergent from the northern subspecies (Salzburger *et al.*, 2002). Previous study based on *P. palustris* cytochrome *b* (Cyt*b*) sequences showed that individuals from Sweden and Siberia were only marginally divergent (Gill *et al.*, 2005). In contrast, *P. p. hypermelaenus*, which is distributed in southwest China to Myanmar, has recently been suggested to be a distinct species (Johansson *et al.*, 2013). All these studies indicate a major genetic divergence in eastern Asia. However, the exact location of the geographical barriers that may have created the phylogeographical divergence of the three species have not been substantially established.

By comparing the phylogeographical structure of the three passerines, we will test: (1) whether congruent genetic breaks can be demonstrated in eastern China; (2) whether such breaks correspond to the proposed boundary between the Sino-Japanese/Palaearctic zones as proposed by Holt *et al.* (2013); (3) whether the genetic population structures reflect similar historical dynamics. This study contributes to the understanding of the evolution of zoogeographical regions in the eastern part of the Eurasian continent.

© 2016 John Wiley & Sons Ltd

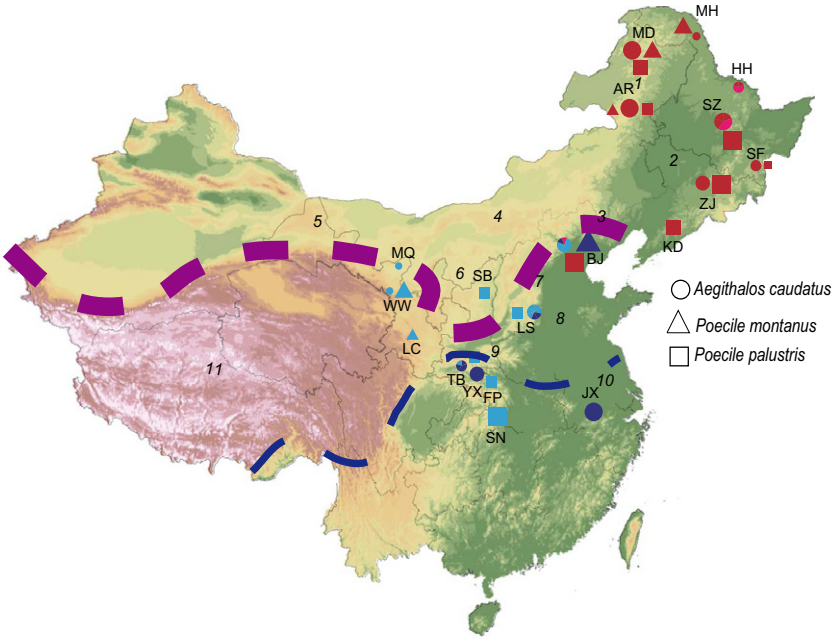

Figure 1 Zoogeographical boundaries and sample information of three woodland bird species in China. Circles, triangles and rectangles represent sampling sites in eastern China, with the size of the symbols being proportional to the number of samples (from 1 to 15). Red, pink, light blue and dark blue represent the major clades identified in Bayesian trees (see coloured bars in Fig. 2). Names of sampling sites are abbreviated (see Table S1 for explanation). Geographical features in China are indicated by italic numbers: *1*, Da Hinggan Ling Mountains; *2*, North-eastern Plain; *3*, Yan Mountains; *4*, Inner Mongolia Plateau; *5*, Gobi Desert; *6*, Loess Plateau; *7*, Taihang Mountains; *8*, North China Plain; *9*, Qinling Mountains; *10*, Middle-Lower Yangtze Plain; *11*, Qinghai-Tibet Plateau. The bold purple dash line indicates the zoogeographical barrier between the Palaearctic and Sino-Japanese realms identified by Holt *et al.* (2013). Narrow dash line in dark blue indicates the traditional Palaearctic/Oriental boundary along the Qinling Mountains – Huai River suggested by Cheng (1987) and Zhang (1999).

MATERIALS AND METHODS

Sample collection and laboratory work

One hundred and one individuals of *P. palustris*, 49 *P. montanus* and 90 *A. caudatus* were collected throughout their distribution in eastern China (Fig. 1; see Table S1). Total DNA was extracted from blood or muscle using the QIAamp DNA Mini Kit (Qiagen, Hilden, Germany). Sequences from two mitochondrial genes (Cytb; NADH dehydrogenase subunit 2, ND2) and three nuclear introns (β-fibrinogen intron 5, Fib5; myoglobin intron 2, Myo2; transforming growth factor beta 2, TGFB2) were amplified using polymerase chain reaction (PCR). The three nuclear introns are widely used in phylogenetic and phylogeographical studies. Although they all evolve more slowly than mitochondrial markers, they have unequal substitution rates (Fib5 is the fastest and Myo2 the slowest). The primer pairs and PCR conditions followed Song *et al.* (2015) but with optimized annealing temperatures.

PCR products were purified with a QIAquick™ PCR purification kit (Qiagen). Sequencing was carried out on an ABI PRISM 3730 automatic sequencer (Applied Biosystems, Foster City, CA, USA) following the ABI PRISM BigDye Terminator Cycle Sequencing protocol. Original sequences were assembled in Seqman II (DNASTAR, Madison, WI, USA). Consensus sequences were aligned using ClustalW in mega 5 (Tamura *et al.*, 2011). The presence of Cytb and ND2 pseudogenes were checked by scanning for stop codons or indels. We used the PHI test in Splitstree4 (Bruen *et al.*, 2006; Huson & Bryant, 2006) and the GARD method (Pond *et al.*, 2006) as implemented in Datamonkey (Pond & Frost, 2005) to search for signatures of recombination in the nuclear sequences. We applied the Phase algorithm (Stephens *et al.*, 2001) in DnaSP 5.0 (Librado & Rozas, 2009) with default parameters to determine the gametic phase of heterozygous nuclear genes. The analysis was run three times with random initiated seeds to check for convergence across replicates. Consistency was confirmed by comparing the haplotype frequencies and goodness of fit values estimated for these runs. Sequences with posterior probabilities larger than 90% were retained for the subsequent analyses. All sequences used in this study were deposited in GenBank (see Table S1).

Genetic analyses for population structure

We concatenated the Cytb and ND2 genes because they are linked and have likely evolved under similar constraints.

© 2016 John Wiley & Sons Ltd

Population genetic parameters, such as the number of segregating sites (S), number of haplotypes (Nhap), haplotype diversity (Hd) and nucleotide diversity (Pi), were determined by DnaSP 5.0. We used MrModeltest 2.3 (Nylander, 2004) to identify the appropriate sequence evolutionary model for each locus.

To investigate lineage divergence within each of the three species, the intraspecific phylogeny based on mitochondrial haplotypes was reconstructed using a constant population size coalescent model in beast 1.8 (Drummond *et al.*, 2012). We set substitution models according to the best-fit model for each species as determined by MrModeltest 2.3. The strict molecular clock model (Drummond *et al.*, 2006) was applied as the sequence substitutions were expected to be constant among intra-specific lineages. The Markov chain Monte Carlo (MCMC) chain was run for more than 100 million generations, with a sampling frequency every 1000 generations. Convergence to the posterior distributions of the parameter estimates was evaluated by monitoring the effective sample size (ESS > 200) and trace plots in Tracer 1.6 (Rambaut *et al.*, 2014). The analyses were carried out on the CIPRES portal (Miller *et al.*, 2010), and we ran the same Beauti file three times to ensure the consistency of the results among the independent runs. A maximum-credibility tree was calculated in treeannotator 1.8 (Drummond *et al.*, 2012) after removing the first 10% of the trees as 'burn-in'. We used the parsimony software tcs 1.21 (Clement *et al.*, 2000) to construct the networks based on combined mitochondrial haplotypes. We set the default at 95% parsimoniously plausible branch connections between haplotypes.

The nuDNA was analysed using *beast (Heled & Drummond, 2010) implemented in beast 2.0 (Bouckaert *et al.*, 2014) to test the lineage divergence revealed in the mtDNA. We unlinked the substitution models across the three introns and set the substitution parameters for each locus according to the MrModeltest results. We chose a piecewise linear population size model with a constant root as the species tree prior, and used the default molecular clock settings (strict clock model, the rate of the first locus = 1.0 and the rates for other loci were to be estimated). The MCMC chains ran for 500 million generations, with sampling every 5000 generations. The convergence of the MCMC chains was examined in Tracer 1.6, and the first 10% were discarded as 'burn-in'. The results were visualized in the software densitree (Bouckaert, 2010). We also used structure 2.3 (Pritchard *et al.*, 2000) to detect the population structure based on the genotype data from the three nuclear introns. An admixture model with correlated allele frequencies was applied, and sampling locality was set *a priori* to magnify the genetic signal (Hubisz *et al.*, 2009). For each species the number of clusters (K) was set from 1 to 10, and each K was run 10 times. The program started with a 'burn-in' of 1×10^5 followed by 1×10^5 MCMC iterations. The K with the highest likelihood was identified by ΔK (Evanno *et al.*, 2005) in Structure Harvester (Earl & Vonholdt, 2012). Clumpp (Jakobsson & Rosenberg, 2007) was used to merge the results of the replicated runs for each K, and Distruct (Rosenberg, 2004) was applied to generate bar plots of the combined results.

The population structure based on concatenated mtDNA sequences was tested in Arlequin 3.11 (Excoffier *et al.*, 2005) by analysis of molecular variance (AMOVA). We tested different grouping arrangements referring to physical barriers (e.g. the Yan and Qinling mountains), subspecies delimitation and phylogenetic results. The statistical significance of the variance components in the AMOVA was tested with 10,000 permutations.

A pairwise F_{ST} was calculated using the corrected average pairwise difference [PiXY−(PiX+PiY)/2] in Arlequin 3.11. Genetic barriers corresponding to abrupt changes in the patterns of genetic variation among the populations were identified in Barrier 2.2 (Manni *et al.*, 2004). The geographical coordinates of each population were connected by Delaunay triangulation, and the corresponding Voronoi tessellation was derived. The maximum difference algorithm (Monmonier, 1973) was used to identify genetic barriers among the populations. Given our aim of identifying any major barrier in eastern China, we tested one genetic barrier using 1000 resampled bootstrap matrices of F_{ST} among the pairs of populations calculated in Arlequin 3.11.

Divergence dating and historical demographic reconstruction

The divergence times were estimated with the same beast methods as above. We accepted the substitution rate (0.0105 site/million years) of the standard molecular clock for Cytb (Weir & Schluter, 2008), and modified the value for the combined mtDNA sequences: We calculated the average overall mean p distances for Cytb and for the combined mtDNA sequences (Cytb and ND2), respectively. The results showed that the average overall mean p distances for the combined mtDNA (0.0126) was 1.19 times of that of Cytb (0.0106). Thus, we obtained a substitution rate of 0.0125 site/million years for the combined mtDNA by multiplying the ratio of 1.19 by the substitution rate of the standard molecular clock for Cytb. The analyses ran under a constant growth model with a strict molecular clock model. Chains were run for 100 million generations with sampling every 1000 generations. We used Tracer 1.6 to monitor the posterior distribution and the ESSs and summarized the posterior probabilities of each parameter after discarding the first 10% of the samples as 'burn-in'.

To assess whether populations have experienced historical fluctuations, we calculated Tajima's D & Fu's F. We used McDonald and Kreitman's method (Mcdonald & Kreitman, 1991) to test for selective neutrality in the mtDNA. We used Bayesian skyline plot (BSP) in beast 1.8 to reconstruct the effective population size fluctuations since the time of the most recent common ancestor (TMRCA). For each lineage, the chains were run for 30 million generations or more until the ESS value

© 2016 John Wiley & Sons Ltd

was larger than 200 after 10% 'burn-in'. The demographic history through time was reconstructed using TRACER 1.6.

To estimate gene flow among the major lineages, we analysed the population parameters in IMa2 (Hey, 2010) with mtDNA and nuDNA sequences respectively. We used the HKY model of evolution for both the mitochondrial and nuclear sequences. The mutation rate for each nuclear locus was estimated by multiplying the ratio of the overall mean *P* distance of each intron with that of Cytb based on the classic molecular clock mutation rate (0.0105 site/million years). Inheritance scalars were set at 1 for the nuclear loci and 0.25 for the mtDNA. The program ran in metropolis coupled MCMC mode with ten chains of linear heating. We first tried multiple times with different prior settings of maximum values for the splitting time (*t*0), population size parameters (q0, q1, q2), and migration parameters ($m_{0>1}$, $m_{1>0}$) to ensure that we reached the likelihood peak for each parameter, then repeated this three times with the final parameter setting but different start seeds. The MCMC chain of each replication ran 10×10^5 steps, with the first 10×10^4 discarded as 'burn-in'. Convergence between the Markov chains at stationary distribution was checked by assessing the ESS > 100, trend line plots, and swapping rates between chains over the course of the run.

RESULTS

Genetic polymorphism and molecular evolutionary properties

We obtained 943 base pairs (bp) of Cytb and 996 bp of ND2 for *P. palustris* and *P. montanus*, and 1011 bp of Cytb and 1014 bp of ND2 for *A. caudatus*. The concatenated mtDNA sequences generated 57, 34 and 75 haplotypes in *P. palustris*, *P. montanus* and *A. caudatus* respectively. *Poecile montanus* had the largest Hd: 0.974, while *P. palustris* had the largest Pi: 0.017. The sequence length of the introns varied among the three species (572–577 bp for Fib5, 733–742 bp for Myo2, and 589–609 bp for TGFB2). *Poecile palustris* had the highest genetic diversity in Fib5, and *P. mon-*

Table 1 Nucleotide polymorphism and results of neutrality tests for three bird species.

	mtDNA			Nuclear DNA		
	Cyt*b*	ND2	Combined	Fib5	Myo2	TGFB2
P. palustris						
Length(bp)	943	996	1939	573	731	589
S	60	73	133	30	15	31
Nhap	45	29	57	31	16	20
Pi	0.016	0.019	0.017	0.007	0.001	0.005
Hd	0.887	0.842	0.966	0.831	0.572	0.483
Overall mean distance	0.016	0.020	0.018	0.009	0.001	0.005
Fu's *F*	−1.692	0.100	−0.789	−0.493	−3.030**	0.261
Tajima's *D*	0.608	1.293	0.998	−0.863	−1.731*	−1.307
MK test	1.600	0.658				
P. montanus						
Length(bp)	943	996	1939	573	733	589
S	36	57	93	20	12	16
Nhap	24	28	34	19	13	22
Pi	0.008	0.015	0.012	0.005	0.001	0.006
Hd	0.905	0.946	0.974	0.830	0.488	0.878
Overall mean distance	0.009	0.016	0.013	0.005	0.001	0.007
Fu's *F*	−1.478	−0.806	−1.138	−0.709	−1.204	0.394
Tajima's *D*	0.122	0.803	0.552	−0.875	−1.181*	0.393
MK test	3.091	1.286				
A. caudatus						
Length(bp)	1011	1014	2025	577	742	609
S	36	39	75	19	6	9
Nhap	22	25	38	21	7	13
Pi	0.007	0.008	0.007	0.003	0.0004	0.0015
Hd	0.842	0.911	0.954	0.651	0.272	0.652
Overall mean distance	0.007	0.008	0.008	0.003	0.000	0.002
Fu's *F*	−0.889	−0.719	−0.877	−0.094	−1.365	−0.677
Tajima's *D*	0.206	0.188	0.206	−1.475	−1.497	−0.975
MK test	3.24	1.772				

*$P < 0.05$, **$P < 0.01$.

S, number of segregating sites; Nhap, number of haplotypes; Hd, haplotype diversity; Pi, nucleotide diversity; Fu's *F*, statistics of Fu's *F* test; Tajima's *D*, statistics of Tajima's *D*-test; MK test, statistics of McDonald and Kreitman's test.

© 2016 John Wiley & Sons Ltd

tanus had the highest genetic diversity in TGFB2. The overall mean pairwise distances were greatest in *P. palustris* for three loci (Cytb 0.016, ND2 0.020 and Fib5 0.009), while the lowest values for all five loci were found in *A. caudatus* (Cytb 0.007, ND2 0.008, Fib5 0.003, Myo2 0.000, and TGFB2 0.002). Neither Tajima's *D* nor Fu's *F* tests showed significant deviations from neutrality for any of the five loci in the three species, except for significant negative Tajima's *D* and Fu's *F* values for Myo2 in *P. palustris* and *P. montanus*. No significant deviation from neutrality was found in Cytb or ND2 according to the McDonald and Kreitman's tests (Table 1).

Intra-specific phylogeny and population structure

The intra-specific phylogenies based on the mitochondrial haplotypes strongly support the geographical divergences between the northern and southern regions of eastern China (Fig. 2). Sub-clades within the major clades were supported by high posterior probabilities in *A. caudatus* (A1, A2 and B1, B2) and *P. montanus* (A, B1 and B2). The TCS networks were congruent with the tree topology in that the haplotype clusters corresponding to the major clades were disconnected (Fig. 2). In *A. caudatus*, some haplotypes from the two clades co-existed in Beijing (BJ). In *P. palustris*, the haplotypes from BJ grouped within the northern clade A, while the haplotypes in *P. montanus* from BJ grouped within the southern clade B (Fig. 1).

The *BEAST analyses recovered intra-specific phylogenies consistent with the mtDNA sequence data in all three species. The major lineages of the north and south (A, B) received high support values (0.99). According to the Structure analyses, the best clustering values were K = 3, 2, and 5 for *P. palustris*, *P. montanus and A. caudatus*, respec-

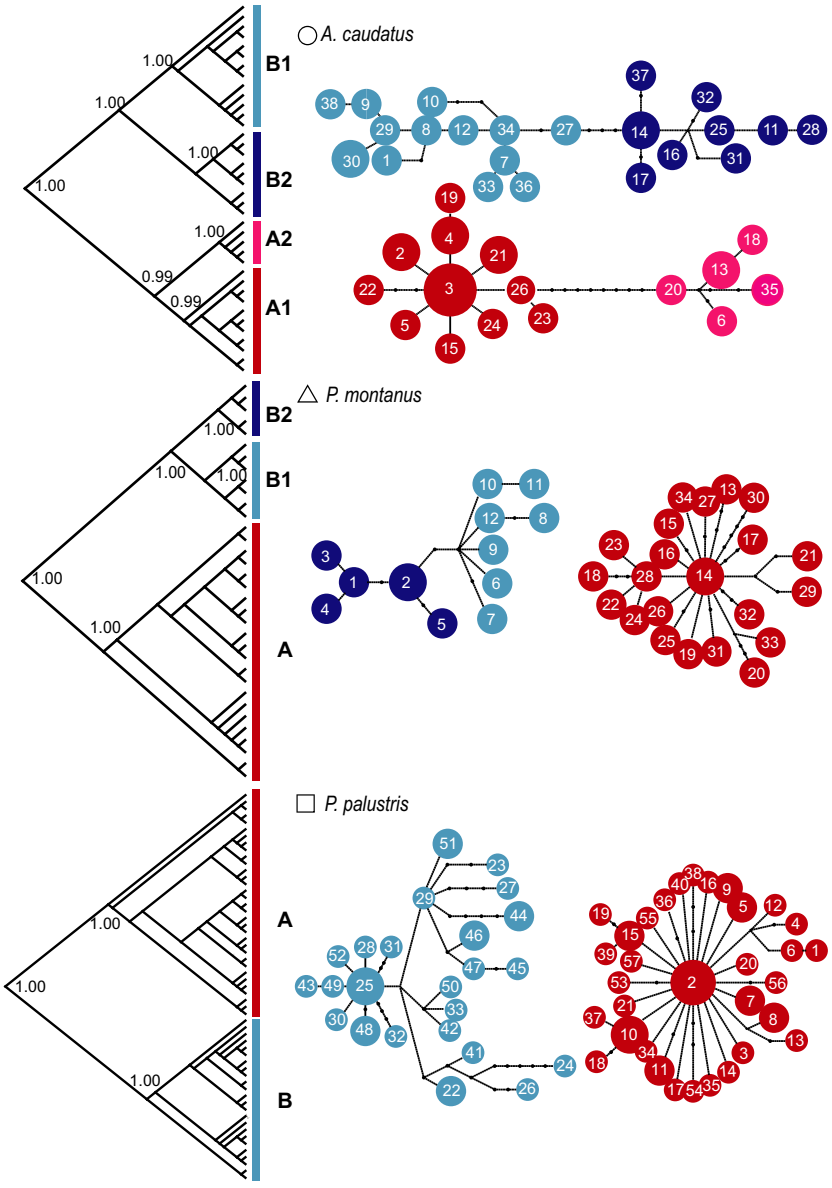

Figure 2 Intra-specific Bayesian trees and TCS networks based on mitochondrial haplotypes. Coloured bars at the tips of the trees represent geographical clades in eastern China: red hues represent clades from north-east China and blue hues clades from central and south China. Posterior probabilities > 0.90 were labelled at each node. Numbered pies in TCS network indicate mitochondrial haplotypes in the phylogenetic tree. Black dots refer to missing steps intermediate between observed haplotypes.

© 2016 John Wiley & Sons Ltd

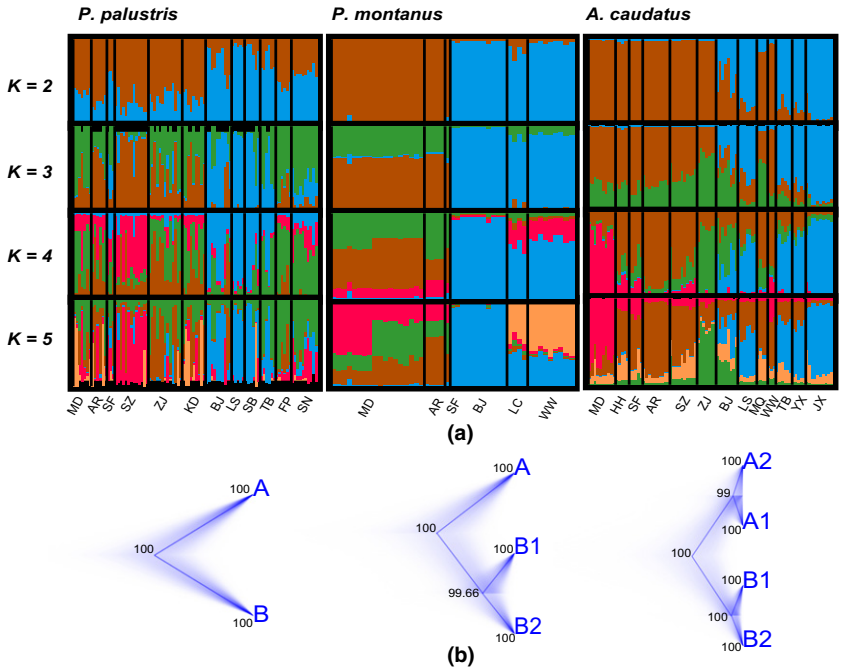

Figure 3 Intra-specific phylogenies and population structures based on nuDNA. (a) Bar plots of *K* values from 2 to 5. Different colours represent pre-set clusters (*K*). Each individual is represented by a column with estimated proportions to each given cluster along the *Y* axis. Codes under the figures show the sampling sites for each bird species (see Fig. 1 and Table S1). (b) *BEAST phylogenies based on three nuclear introns. Cloudograms show all trees from analyses; darker branches represent a greater proportion of corresponding trees. Consensus trees are presented by solid lines, and posterior probabilities are shown at the nodes.

Table 2 AMOVA results based on mtDNA for three bird species.

Grouping	Source of variation	d.f.	Percentage of variation
P. palustris (AR, KD, MD, SF, SZ, ZJ/BJ, FP, LS, SB, SN, TB)	Among groups	1	95.16
	Among populations within groups	10	0.43
	Within populations	89	4.41
P. montanus (AR, MD, SF/BJ/LC, WW)	Among groups	2	91.16
	Among populations within groups	4	1.04
	Within populations	42	7.08
A. caudatus (AR, HH, MD, SF, SZ, ZJ/BJ/LS/MQ, WW/JX, TB, YX)	Among groups	4	78.59
	Among populations within groups	8	4.53
	Within populations	77	16.88

tively. When $K = 2$, the bar plots showed a consistent pattern of north/south differentiation. However, the degree of north/south differentiation varied among the three species. *Poecile palustris* was only slightly differentiated, and the southern populations Foping (FP) and Shennongjia (SN) had similar cluster components to the northern populations. When *K* was larger than 2, the *A. caudatus* populations from Minqin (MQ) and Wuwei (WW) showed a closer relationship with populations from north-eastern China, while the westernmost *P. montanus* populations, Liancheng (LC) and WW, formed an independent cluster (Fig. 3).

AMOVA showed a maximum percentage of among-group variance (95.16%) in *P. palustris* when the populations were grouped as north and south. In *P. montanus*, a further division of BJ/LC & WW led to the highest among-group variance (91.16%). In *A. caudatus*, five geographical groups were identified, with a maximum variance percentage of 78.59% (Table 2).

The F_{ST} matrices based on mtDNA identified a congruent barrier among the three species near sampling locality BJ. The same geographical barrier was also recorded in the F_{ST} values of Fib5 and TGFB2 in *P. montanus*, whereas in the other two species, the geographical barriers varied randomly depending on the introns used (Fig. 4).

Divergence time and demographic dynamics

The divergence times between the two major clades (north/south) differed among the species (Fig. 5). *P. palustris* had the earliest divergence time, *c.* 1.94 million years ago (Ma) and the 95% highest probability density (95% HPD) was 1.37–2.55 Ma. The divergence times in *P. montanus* and *A. caudatus* were *c.* 0.98 (95% HPD: 0.73–1.26 Ma) and 0.57 (95% HPD: 0.39–0.76 Ma).

The BSP showed a similar pattern in all three species, as the northern lineage (clade A) had a shorter population history than the southern counterpart (clade B). The TMRCA

© 2016 John Wiley & Sons Ltd

for the northern clade was 0.07 (95% HPD: 0.05–0.11 Ma), 0.09 (95% HPD: 0.06–0.14 Ma), and 0.23 (95% HPD: 0.12–0.34 Ma) for *P. palustris*, *P. montanus* and *A. caudatus* respectively; for the southern clade, it was 0.14 (95% HPD: 0.08–0.19 Ma), 0.10 (95% HPD: 0.05–0.16 Ma), and 0.17 (95% HPD: 0.09–0.25 Ma). Recent population expansions were dated at *c.* 0.06 Ma, with a greater change in *P. palustris* and *A. caudatus* than in *P. montanus*. The southern lineages have fluctuated less through time than the northern lineages (Fig. 6).

Bidirectional migration rates were rather small in the mtDNA in all three species. In *P. palustris*, the highest posterior density values (HiPt) and 95% HPD were 0.00 (0.00–0.07) migrants/generation from south to north and 0.00 (0.00–0.08) migrants/generation from north to south. In *P. montanus*, the south–north gene flow was 0.00 (0.00–0.33) migrants/generation; the north–south gene flow was 0.00 (0.00–0.17) migrants/generation. In *A. caudatus*, the south–north gene flow was 0.00 (0.00–0.07) migrants/generation; the north–south gene flow was 0.00 (0.00–0.17) migrants/generation. Asymmetric gene flow was recorded in the nuclear introns for *P. montanus* and *A. caudatus*. In *P. montanus*, greater migration rates were found from north to south [0.35 (0.06–2.40) migrants/generation] than from south to north [0.13 (0.02–0.59) migrants/generation]. In contrast, *A. caudatus* had more migrants from south to north [2.41 (0.98–5.91) migrants/generation] than in the opposite direction [0.02 (0.02–1.95) migrants/generation]. However,

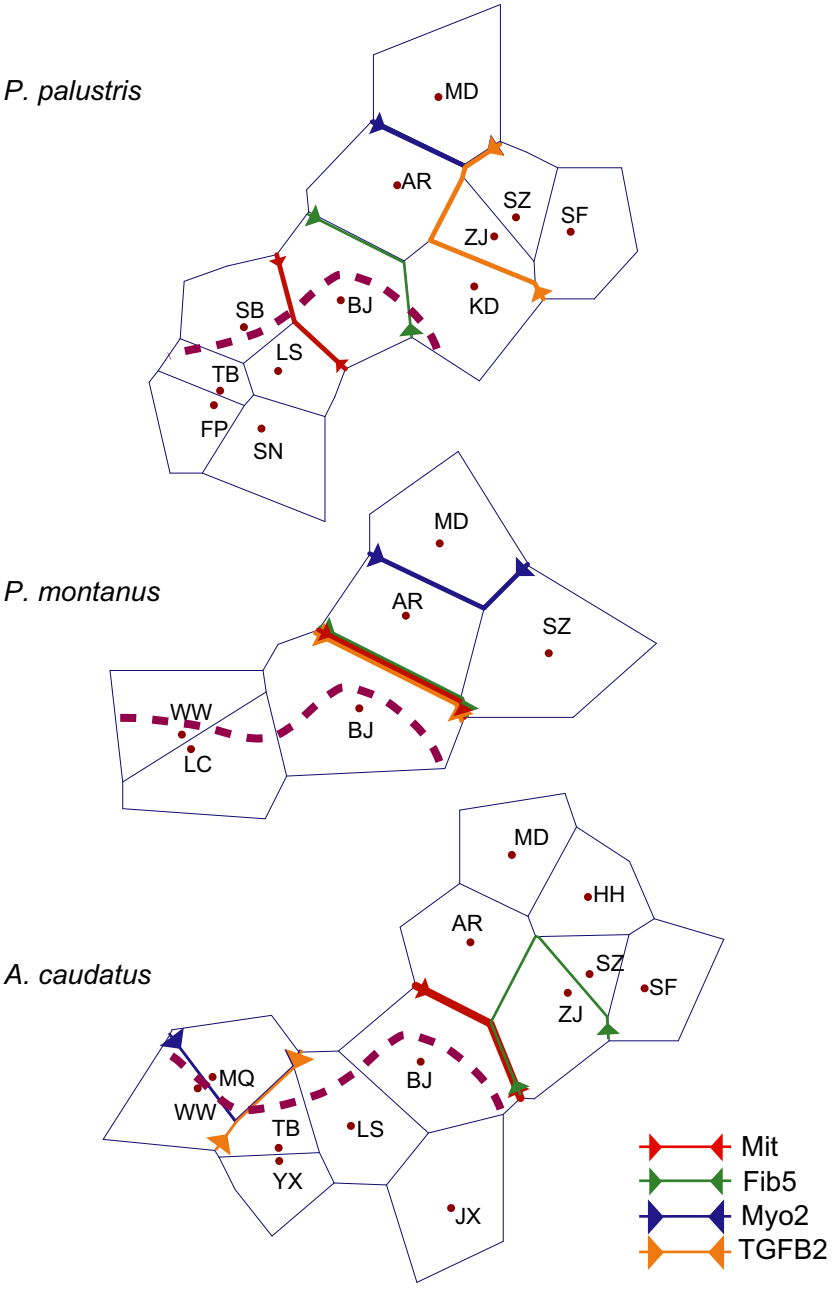

Figure 4 Geographical barriers identified by mitochondrial and nuclear loci in three bird species. Coloured stripe indicates the major barrier determined by maximum difference algorithm in BARRIER 2.2 based on F_{ST} differences. The purple dash line represents the expected major genetic barrier among populations according to the boundary between the Palaearctic and Sino-Japanese realms identified by Holt *et al.* (2013).

© 2016 John Wiley & Sons Ltd

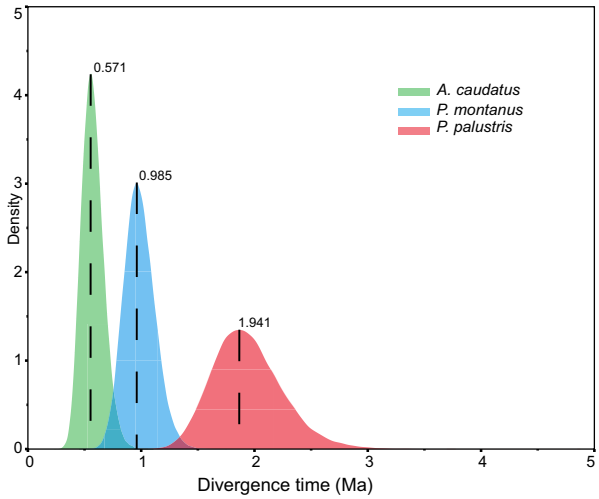

Figure 5 Estimation of lineage divergence times based on mtDNA. The *X* axis is the time prior of the lineage divergence event, the *Y* axis is the density of poster probability summarized by Tracer based on Markov chain Monte Carlo simulations generated by beast 1.8. Dash line and number above each curve show mean value of divergence time for each species.

due to the overlap in the 95% HPDs of migrants, asymmetrical gene flow could not be confidently confirmed in *P. montanus* (Fig. 7; see Table S2).

DISCUSSION

Congruent patterns of north/south population divergence in eastern China

All three species in our study span a wide geographical area across the Eurasian continent. Previous studies have suggested that the *A. caudatus* populations from the northern Palaearctic, including north-eastern China, are sister taxa to those from southern China (Päckert *et al.*, 2010; Song *et al.*, 2015). A more complex pattern has been revealed in *P. montanus* and the central Chinese populations were deeply divergent from the northern Palaearctic ones (Kvist *et al.*, 2001; Salzburger *et al.*, 2002). In *P. palustris*, the deep divergence between the lineages from north-eastern (*P. p. brevirostris*) and south-western (*P. p. hypermelaenus*) China suggested by Johansson *et al.* (2013) was supported by our results. For all three species, both the mitochondrial and the nuclear data sets strongly support the presence of a major divergence between the northern and southern populations. This is evident from the trees, networks as well as the barrier inferences. Barrier results suggest that the border is approximately at the latitude of BJ. The results are consistent with previous studies on some other organisms (Zhang *et al.*, 2008; Bai *et al.*, 2010; Sakka *et al.*, 2010; Ding *et al.*, 2011). These congruent indications of north/south genetic divergences demonstrate a long-lasting barrier to many organisms in the north Hebei, Beijing and south Liaoning provinces at *c.* 40° N.

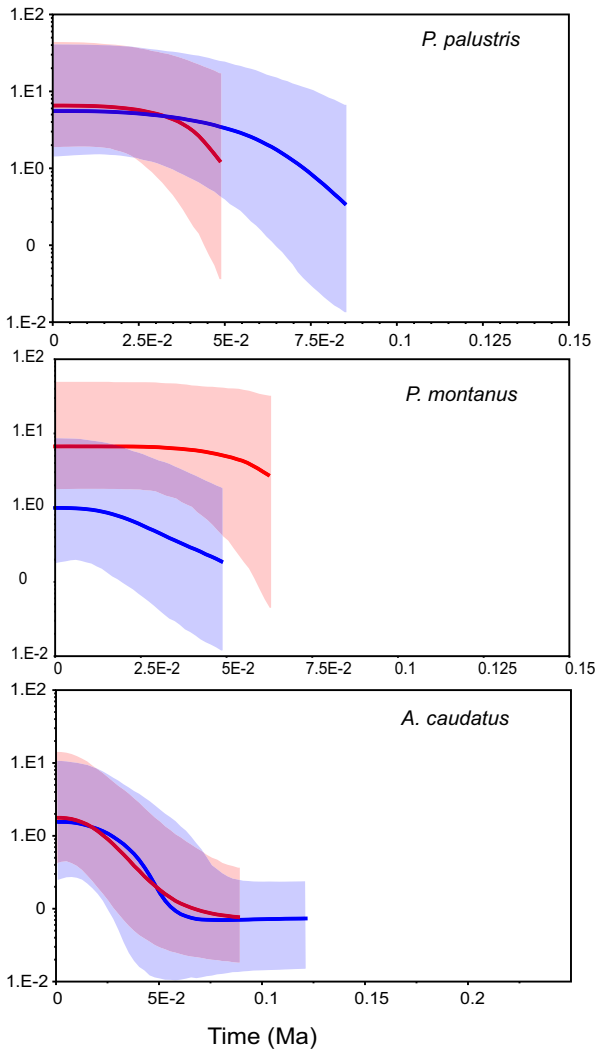

Figure 6 Bayesian skyline plot for historical demographic trends of major lineages in each species. The *X* axis is the time-scale before present in units of million years ago, and the *Y* axis is the estimated effective population size. Estimates of means are joined by a solid line while the shaded range delineates the 95% HPD limits. Red colour represents north lineages and blue south lineages.

We propose that several geographical and environmental factors have contributed to the existence of such barriers. First, the phylogeographical breaks coincide with the Yan Mountains (*3* in Fig. 1), one of the principal mountain ranges in eastern China, with a mainly east-west extension and the highest peaks more than 2100 m. The uplift of the Yan Mountains occurred much earlier in the Jurassic–Cretaceous period (Davis *et al.*, 2001; Deng *et al.*, 2004). Montane forests were replaced by steppe and tundra grasslands during the glacial periods of the Pleistocene (Xu *et al.*, 2002). The topographical complexity of the montane region and the vegetation transformation during the cold and dry periods likely restricted the dispersal of these sedentary species.

Second, the eco-climatic changes in north China may have contributed to barrier effects that influenced these woodland

© 2016 John Wiley & Sons Ltd

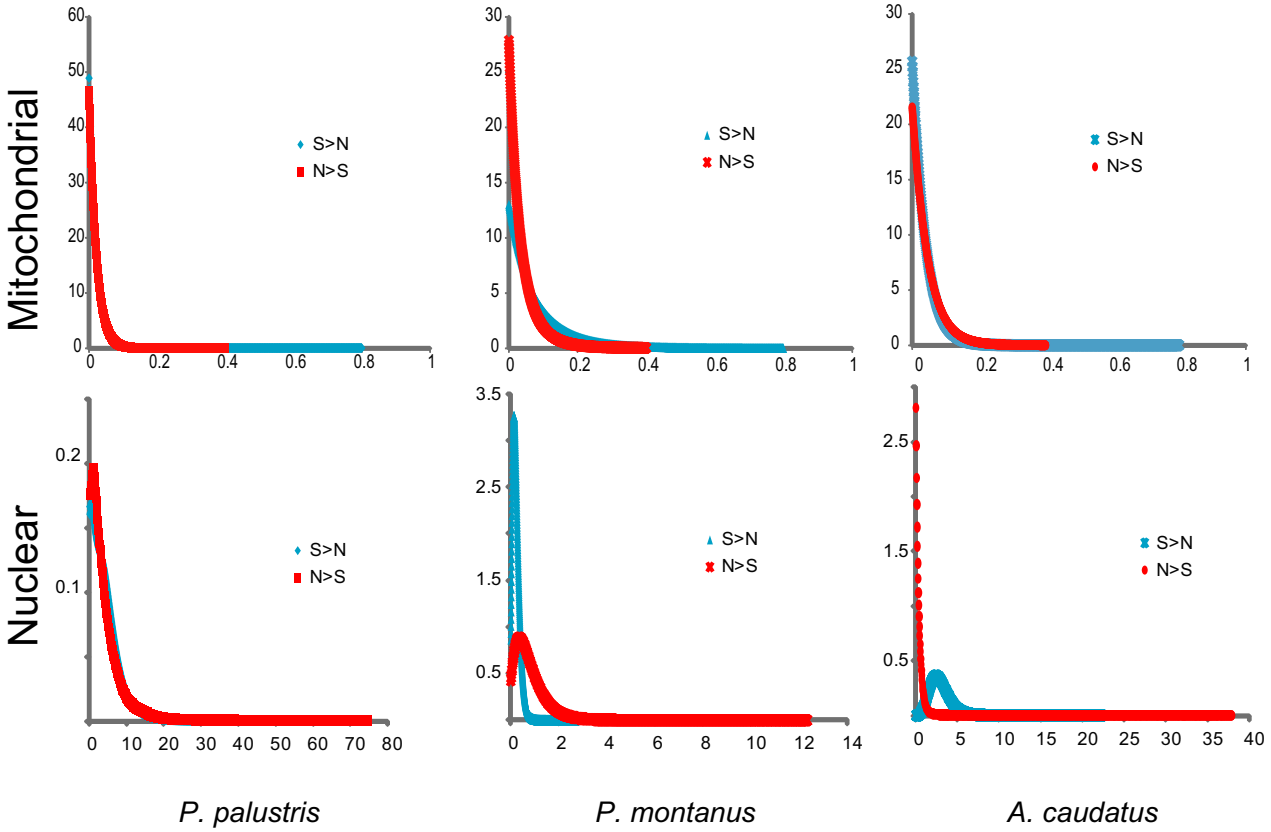

Figure 7 Posterior probability density distributions of migration rates (2NM) based on mitochondrial and nuclear DNA. *X* axis represents the prior distribution of the migration rate (m), *Y* axis marginal posterior probability density distribution. N>S represents the migration rate from the northern lineage to the southern lineage in each species; S>N represents the migration rate from the south to the north. Parameter estimates are scaled to the mutation rate.

avian species. The uplifting of the Qinghai-Tibet Plateau and the glacial extension during the Pleistocene would likely have induced the expansion of steppe grasslands and even the origin of arid conditions, which replaced the forests (Cheng, 2000; An *et al.*, 2001; Harrison *et al.*, 2001). We propose that the loss of favoured woodland habitats might have contributed to the separation between the northern and southern populations in eastern China. Two other species, *Phasianus colchicus* and *Pica pica*, which depend less on forested areas than the three woodland species of this study, do not show a similar deep divergence (Liu *et al.*, 2010; Zhang *et al.*, 2012). However, the foraging and breeding behaviour of the three species largely depend on dense vegetation. We therefore suggest that habitat discontinuities in the past may have restricted the gene flow and driven population divergence.

Variation in lineage divergence times between north/south populations and gene-flow directions across the zoogeographical boundary

Poecile montanus and *A. caudatus* both diverged around the boundary between the Calabrian and Middle Pleistocene (0.93 and 0.80 Ma respectively). This divergence corresponds to the onset of large-amplitude glacial cycles in the Northern Hemisphere (Krantz, 1991; Head & Gibbard, 2005). The lineage divergence within *P. palustris* occurred somewhat earlier in the early Pleistocene (1.94 Ma). These results imply that the north/south divergences may have happened several times during different stages of the Pleistocene, demonstrating a long-lasting barrier in the northern part of eastern China.

The Tajima's *D* and Fu's *F* values indicate that the three species were less likely to have experienced strong selective pressures or population declines in response to the climatic shifts in the late Pleistocene. The BSP shapes also show constant population growth through the late Pleistocene. In each species, the TMRCA is earlier in the southern clade than in the north, potentially indicating a more stable environment in the southern part of China. In the northern lineages of the three species, a more significant population growth was observed in *P. palustris*, whereas *P. montanus* had a more stable population size than the other two species. All three species are residents and can withstand extremely low temperatures and harsh winter conditions. *Poecile montanus* prefers coniferous forests in the northern parts of its range, while *P. palustris* mostly inhabits mixed and broadleaved forests (Song, 1980; Fang & Ding, 1997; Yi *et al.*, 2008). The

© 2016 John Wiley & Sons Ltd

persistence of coniferous forests during the glacial periods may have led to a more stable population size in *P. montanus* compared to *P. palustris*.

The gene flow between the northern and southern lineages implies different patterns among the three species. In *P. palustris,* bidirectional gene flow was mostly restricted, whereas for the nuDNA more migrants were inferred from north to south than the reverse. In *P. montanus*, nuDNA showed more migrants moving from the northern population towards the south. Asymmetric migration was also observed in *A. caudatus*, but more from the south to the north, indicating an alternative direction of population expansion between the lineages compared to *P. montanus*. However, the results should be interpreted with caution, as the 95% HPDs of bi-directional nuclear migrants overlapped in *P. palustris* and *P. montanus*.

Rethinking the zoogeographical boundary in eastern China from a phylogeographical viewpoint

The zoogeographical boundary is not only a physical barrier, which might play a role in restricting individuals dispersal, but also reflects different environmental characteristics and selective filters between the two sides of the boundary (Glor & Warren, 2011). The zoogeographical regionalization in eastern China and the location of the zoogeographical boundary has long been the subject of debate (Wallace, 1876; Cheng, 1987; Zhang, 1999; Tan, 2011; Procheş & Ramdhani, 2012; Holt *et al.*, 2013; Kreft & Jetz, 2013; Rueda *et al.*, 2013). Wallace (1876) suggested a subtropical location for the Palaearctic/Oriental boundary. More recently, this has also been emphasized by others for birds and mammals (Cheng, 1987; Zhang, 1999; Tan, 2011; Zhang *et al.*, 2014), although the boundary has been located slightly more to the south than suggested by Holt *et al.* (2013). However, the three species in our study show phylogeographical breaks in the northern part of eastern China, supporting the zoogeographical boundary proposed by Holt *et al.* (2013). We propose that the barrier effects of the Yan Mountains combined with the climatic and vegetational substitution during the Pleistocene, support the validity of the Palaearctic/Sino-Japanese boundary of Holt *et al.* in delineating the regional faunal transition in eastern China.

ACKNOWLEDGEMENTS

We thank Chuanyin Dai at Guizhou Normal College and Xuebin Gao and Kaifeng Wang at the Shaanxi Institute of Zoology for their help in the fieldwork. We are grateful to the editor and three anonymous reviewers for their valuable comments. The project was funded by the State Key Program of NSFC (31330073) and Major International (Regional) Joint Research Project (31010103901) to F.L., MOST Grant (2011FY120200) to Y.Q., NSFC funds to G.S. (31101630 & 31471991), and Swedish Research Council funding (621-2013-5161) to P.G.P.E. A.K. thanks the Scientific Grant Agency VEGA (2/0097/16). P.A. acknowledges the Chinese Academy of Sciences Visiting Professorship for Senior International Scientists (2011T2S04) and The Sound Approach. J.F. thanks the Danish National Research Foundation for support to the Centre for Macroecology, Evolution and Climate.

REFERENCES

An, Z.S., Kutzbach, J.E., Prell, W.L. & Porter, S.C. (2001) Evolution of Asian monsoons and phased uplift of the Himalayan Tibetan plateau since Late Miocene times. *Nature*, **411**, 62–66.

Arbogast, B.S. & Kenagy, G.J. (2001) Comparative phylogeography as an integrative approach to historical biogeography. *Journal of Biogeography*, **28**, 819–825.

Avise, J.C. (1992) Molecular population structure and the biogeographic history of a regional fauna: a case history with lessons for conservation biology. *Oikos*, **63**, 62–76.

Bai, W.N., Liao, W.J. & Zhang, D.Y. (2010) Nuclear and chloroplast DNA phylogeography reveal two refuge areas with asymmetrical gene flow in a temperate walnut tree from East Asia. *New Phytologist*, **188**, 892–901.

Bouckaert, R., Heled, J., Kuhnert, D., Vaughan, T., Wu, C.H., Xie, D., Suchard, M.A., Rambaut, A. & Drummond, A.J. (2014) BEAST 2: A Software Platform for Bayesian Evolutionary Analysis. *Plos Computational Biology*, **10**.

Bouckaert, R.R. (2010) DensiTree: making sense of sets of phylogenetic trees. *Bioinformatics*, **26**, 1372–1373.

Bruen, T.C., Philippe, H. & Bryant, D. (2006) A simple and robust statistical test for detecting the presence of recombination. *Genetics*, **172**, 2665–2681.

Burton, R.S. (1998) Intraspecific phylogeography across the Point Conception biogeographic boundary. *Evolution*, **52**, 734–745.

Cheng, J. (2000) Research on the early Pleistocene climatic and biotic events in north China – evidence from mammalian faunas. *Geological Science and Technology Information*, **19**, 5–10.

Cheng, T. (1987) *A synopsis to the avifauna of China*. Science Press, Beijing.

Clement, M., Posada, D. & Crandall, K.A. (2000) TCS: a computer program to estimate gene genealogies. *Molecular Ecology*, **9**, 1657–1659.

Davis, G.A., Zheng, Y.D., Wang, C., Darby, B.J. & Zhang, C.H. (2001) Mesozoic tectonic evolution of the Yanshan fold and thrust belt, with emphasis on Hebei and Liaoning provinces, northern China. *Paleozoic and Mesozoic Tectonic Evolution of Central Asia: From Continental Assembly to Intracontinental Deformation*, **194**, 171–197.

Deng, J.F., Su, S.G., Mo, X.X., Zhao, G.C., Xiao, Q.H. & Ji, G.Y. (2004) The sequence of magmatic-tectonic events and orogenic processes of the Yanshan Belt, North China. *Acta Geologica Sinica-English Edition*, **78**, 260–266.

© 2016 John Wiley & Sons Ltd

Ding, L., Gan, X.N., He, S.P. & Zhao, E.M. (2011) A phylogeographic, demographic and historical analysis of the short-tailed pit viper (*Gloydius brevicaudus*): evidence for early divergence and late expansion during the Pleistocene. *Molecular Ecology*, **20**, 1905–1922.

Drummond, A.J., Ho, S.Y.W., Phillips, M.J. & Rambaut, A. (2006) Relaxed phylogenetics and dating with confidence. *Plos Biology*, **4**, 699–710.

Drummond, A.J., Suchard, M.A., Xie, D. & Rambaut, A. (2012) Bayesian phylogenetics with BEAUti and the BEAST 1.7. *Molecular Biology and Evolution*, **29**, 1969–1973.

Earl, D.A. & Vonholdt, B.M. (2012) STRUCTURE HARVESTER: a website and program for visualizing structure output and implementing the Evanno method. *Conservation Genetics Resources*, **4**, 359–361.

Eberl, R., Mateos, M., Grosberg, R.K., Santamaria, C.A. & Hurtado, L.A. (2013) Phylogeography of the supralittoral isopod *Ligia occidentalis* around the Point Conception marine biogeographical boundary. *Journal of Biogeography*, **40**, 2361–2372.

Evanno, G., Regnaut, S. & Goudet, J. (2005) Detecting the number of clusters of individuals using the software STRUCTURE: a simulation study. *Molecular Ecology*, **14**, 2611–2620.

Excoffier, L., Laval, G. & Schneider, S. (2005) Arlequin ver. 3.0: an integrated software package for population genetics data analysis. *Evolutionary Bioinformatics Online*, **1**, 47–50.

Fang, C. & Ding, Y. (1997) The breeding ecology of the *Aegithalos caudatus glaucogularis* (in Chinese). *Chinese Journal of Zoology*, **32**, 14–16.

Gill, F. & Donsker, D. (eds) (2015) *IOC world bird list (v 5.4)*. doi:10.14344/IOC.ML.5.4.

Gill, F.B., Slikas, B. & Sheldon, F.H. (2005) Phylogeny of titmice (Paridae): II. Species relationships based on sequences of the mitochondrial cytochrome-b gene. *The Auk*, **122**, 121–143.

Glor, R.E. & Warren, D. (2011) Testing ecological explanations for biogeographic boundaries. *Evolution*, **65**, 673–683.

Gosler, A. & Clement, P. (2007) Marsh Tit (*Poecile palustris*) & Willow Tit (*Poecile montanus*). *Handbook of the birds of the world* (ed. by J. Del Hoyo, A. Elliott, J. Sargatal, D.A. Christie and E. De Juana). pp. 711–713. Lynx Edicions, Barcelona.

Harrap, S. (2008) Family Aegithalidae (long-tailed tits). *Handbook of the birds of the world* (ed. by J. Del Hoyo, A. Elliott, J. Sargatal, D.A. Christie and E. De Juana). pp. 95–96. Lynx Edicions, Barcelona.

Harrison, S.P., Yu, G., Takahara, H. & Prentice, I.C. (2001) Palaeovegetation. Diversity of temperate plants in east Asia. *Nature*, **413**, 129–130.

Head, M.J. & Gibbard, P.L. (2005) Early-Middle Pleistocene transitions: an overview and recommendation for the defining boundary. *Geological Society, London, Special Publications*, **247**, 1–18.

Heled, J. & Drummond, A.J. (2010) Bayesian Inference of Species Trees from Multilocus Data. *Molecular Biology and Evolution*, **27**, 570–580.

Hey, J. (2010) Isolation with migration models for more than two populations. *Molecular Biology and Evolution*, **27**, 905–920.

Holt, B., Lessard, J.P., Borregaard, M.K., Fritz, S.A., Araujo, M.B., Dimitrov, D., Fabre, P.H., Graham, C.H., Graves, G.R., Jonsson, K.A., Nogues-Bravo, D., Wang, Z.H., Whittaker, R.J., Fjeldsa, J. & Rahbek, C. (2013) An update of Wallace's zoogeographic regions of the world. *Science*, **339**, 74–78.

Hubisz, M.J., Falush, D., Stephens, M. & Pritchard, J.K. (2009) Inferring weak population structure with the assistance of sample group information. *Molecular Ecology Resources*, **9**, 1322–1332.

Huson, D.H. & Bryant, D. (2006) Application of phylogenetic networks in evolutionary studies. *Molecular Biology and Evolution*, **23**, 254–267.

Jakobsson, M. & Rosenberg, N.A. (2007) CLUMPP: a cluster matching and permutation program for dealing with label switching and multimodality in analysis of population structure. *Bioinformatics*, **23**, 1801–1806.

Johansson, U.S., Ekman, J., Bowie, R.C.K., Halvarsson, P., Ohlson, J.I., Price, T.D. & Ericson, P.G.P. (2013) A complete multilocus species phylogeny of the tits and chickadees (Aves: Paridae). *Molecular Phylogenetics and Evolution*, **69**, 852–860.

Krantz, D.E. (1991) A chronology of Pliocene sea-level fluctuations – the United-States middle Atlantic coastal-plain record. *Quaternary Science Reviews*, **10**, 163–174.

Kreft, H. & Jetz, W. (2010) A framework for delineating biogeographical regions based on species distributions. *Journal of Biogeography*, **37**, 2029–2053.

Kreft, H. & Jetz, W. (2013) Comment on 'An update of Wallace's zoogeographical regions of the World'. *Science*, **341**, 343.

Kvist, L., Martens, J., Ahola, A. & Orell, M. (2001) Phylogeography of a Palaearctic sedentary passerine, the willow tit (*Parus montanus*). *Journal of Evolutionary Biology*, **14**, 930–941.

Lei, F.M., Qu, Y.H., Song, G., Alstrom, P. & Fjeldsa, J. (2015) The potential drivers in forming avian biodiversity hotspots in the East Himalaya Mountains of South-west China. *Integrative Zoology*, **10**, 171–181.

Librado, P. & Rozas, J. (2009) DnaSP v5: a software for comprehensive analysis of DNA polymorphism data. *Bioinformatics*, **25**, 1451–1452.

Liu, Y., Zhan, X.J., Wang, N., Chang, J. & Zhang, Z.W. (2010) Effect of geological vicariance on mitochondrial DNA differentiation in Common Pheasant populations of the Loess Plateau and eastern China. *Molecular Phylogenetics and Evolution*, **55**, 409–417.

Manni, F., Guerard, E. & Heyer, E. (2004) Geographic patterns of (genetic, morphologic, linguistic) variation: How barriers can be detected by using Monmonier's algorithm. *Human Biology*, **76**, 173–190.

© 2016 John Wiley & Sons Ltd

Mcdonald, J.H. & Kreitman, M. (1991) Adaptive protein evolution at the Adh locus in Drosophila. *Nature*, **351**, 652–654.

Miller, M.A., Pfeiffer, W. & Schwartz, T. (2010) Creating the CIPRES Science Gateway for inference of large phylogenetic trees. *Proceedings of Gateway Computing Environments Workshop (GCE), 14 November 2010*, pp. 1–8. LA, USA, New Orleans.

Monmonier, M.S. (1973) Maximum-difference barriers: an alternative numerical regionalization method. *Geographical Analysis*, **5**, 245–261.

Nylander, J.A.A. (2004) *MrModeltest v2*. Program distributed by the author. Evolutionary Biology Centre, Uppsala University, Uppsala, Sweden.

Päckert, M., Martens, J. & Sun, Y.H. (2010) Phylogeny of long-tailed tits and allies inferred from mitochondrial and nuclear markers (Aves: Passeriformes, Aegithalidae). *Molecular Phylogenetics and Evolution*, **55**, 952–967.

Päckert, M., Martens, J., Sun, Y.-H., Severinghaus, L.L., Nazarenko, A.A., Ting, J., Toepfer, T. & Tietze, D.T. (2012) Horizontal and elevational phylogeographic patterns of Himalayan and Southeast Asian forest passerines (Aves: Passeriformes). *Journal of Biogeography*, **39**, 556–573.

Pond, S.L.K. & Frost, S.D.W. (2005) Datamonkey: rapid detection of selective pressure on individual sites of codon alignments. *Bioinformatics*, **21**, 2531–2533.

Pond, S.L.K., Posada, D., Gravenor, M.B., Woelk, C.H. & Frost, S.D.W. (2006) Automated phylogenetic detection of recombination using a genetic algorithm. *Molecular Biology and Evolution*, **23**, 1891–1901.

Pritchard, J.K., Stephens, M. & Donnelly, P. (2000) Inference of population structure using multilocus genotype data. *Genetics*, **155**, 945–959.

Procheş, S. & Ramdhani, S. (2012) The world's zoogeographical regions confirmed by cross-taxon analysis. *BioScience*, **62**, 260–270.

Rambaut, A., Suchard, M.A., Xie, D. & Drummond, A.J. (2014) *Tracer v1.6*. Available at: http://beast.bio.ed.ac.uk/Tracer.

Rosenberg, N.A. (2004) DISTRUCT: a program for the graphical display of population structure. *Molecular Ecology Notes*, **4**, 137–138.

Rueda, M., Rodriguez, M.A. & Hawking, B.A. (2013) Identifying global zoogeographical regions: lessons from Wallace. *Journal of Biogeography*, **40**, 2215–2225.

Sakka, H., Quere, J.P., Kartavtseva, I., Pavlenko, M., Chelomina, G., Atopkin, D., Bogdanov, A. & Michaux, J. (2010) Comparative phylogeography of four *Apodemus* species (Mammalia: Rodentia) in the Asian Far East: evidence of Quaternary climatic changes in their genetic structure. *Biological Journal of the Linnean Society*, **100**, 797–821.

Salzburger, W., Martens, J., Nazarenko, A.A., Sun, Y.-H., Dallinger, R. & Sturmbauer, C. (2002) Phylogeography of the Eurasian Willow Tit (*Parus montanus*) based on DNA sequences of the mitochondrial cytochrome b gene. *Molecular Phylogenetics and Evolution*, **24**, 26–34.

Song, G., Zhang, R., DuBay, S.G., Qu, Y., Dong, L., Wang, W., Zhang, Y., Lambert, D.M. & Lei, F. (2015). East Asian allopatry and north Eurasian sympatry in Long-tailed Tit lineages despite similar population dynamics during the late Pleistocene. *Zoologica Scripta*, **45**, 115–126.

Song, Y. (1980) Studies on the breeding ecology and feeding habits of willow tits (in Chinese). *Acta Zoologica Sinica*, **26**, 370–377.

Stephens, M., Smith, N.J. & Donnelly, P. (2001) A new statistical method for haplotype reconstruction from population data. *American Journal of Human Genetics*, **68**, 978–989.

Tamura, K., Peterson, D., Peterson, N., Stecher, G., Nei, M. & Kumar, S. (2011) MEGA5: molecular evolutionary genetics analysis using maximum likelihood, evolutionary distance, and maximum parsimony methods. *Molecular Biology and Evolution*, **28**, 2731–2739.

Tan, Z. (2011) *The calculation and simulation of Chinese South – North demarcation based on GIS (in Chinese)*. Master Thesis, Lanzhou University, Lanzhou.

Wallace, A.R. (1876) *The geographical distribution of Animals*. Cambridge University Press, Cambridge.

Weir, J.T. & Schluter, D. (2008) Calibrating the avian molecular clock. *Molecular Ecology*, **17**, 2321–2328.

Xu, Q., Yang, X., Ke, Z., Liang, W. & Yang, Z. (2002) Environment changes in Yanshan Mountain Area during the Latest Pleistocene (in Chinese). *Geography and Territorial Research*, **18**, 69–72.

Yi, G., Zhao, J., Gao, W., Yang, Z. & Liu, Y. (2008) Breeding ecology of *Parus palustris* brevirostris in secondary forest (in Chinese). *Journal of North-east Forestry University*, **36**, 51–52.

Zhang, F., Yu, D., Luo, Y., Ho, S.Y.W., Wang, B. & Zhu, C. (2014) Cryptic diversity, diversification and vicariance in two species complexes of Tomocerus (Collembola, Tomoceridae) from China. *Zoologica Scripta*, **43**, 393–404.

Zhang, H., Yan, J., Zhang, G. & Zhou, K. (2008) Phylogeography and demographic history of chinese black-spotted frog Populations (*Pelophylax nigromaculata*): evidence for independent refugia expansion and secondary contact. *BMC Evolutionary Biology*, **8**, 21.

Zhang, R. (1999) *Zoogeography of China (in Chinese)*. Science Press, Beijing.

Zhang, R.Y., Song, G., Qu, Y.H., Alström, P., Ramos, R., Xing, X.Y., Ericson, P.G.P., Fjeldsa, J., Wang, H.T., Yang, X.J., Kristin, A., Shestopalov, A.M., Choe, J.C. & Lei, F.M. (2012) Comparative phylogeography of two widespread magpies: importance of habitat preference and breeding behavior on genetic structure in China. *Molecular Phylogenetics and Evolution*, **65**, 562–572.

Zhao, N., Dai, C., Wang, W., Zhang, R., Qu, Y., Song, G., Chen, K., Yang, X., Zou, F. & Lei, F. (2012) Pleistocene climate changes shaped the divergence and demography of Asian populations of the great tit *Parus major*: evidence from phylogeographic analysis and ecological niche models. *Journal of Avian Biology*, **43**, 297–310.

© 2016 John Wiley & Sons Ltd

Zink, R.M., Pavlova, A., Drovetski, S. & Rohwer, S. (2008) Mitochondrial phylogeographies of five widespread Eurasian bird species. *Journal of Ornithology*, **149**, 399–413.

SUPPORTING INFORMATION

Additional Supporting Information may be found in the online version of this article:

Table S1 Sample list of the three species involved in this study.
Table S2 Demographic parameters estimated with IMa2.

DATA ACCESSIBILITY

Sample information and GenBank accession numbers for all sequenced individuals are given in Table S1.

BIOSKETCH

Gang Song is a researcher in the Ornithological Research Group, Institute of Zoology, Chinese Academy of Sciences. His major research interests are in biogeography, phylogeography and population genetics of birds. He is involved in a series of phylogeographical studies on Eurasian passerines. The present paper is part of the results of a comparative phylogeographical study on Eurasian birds, which is a joint international cooperation research project led by F.L., Y.Q., P.A., J.F., P.G.P.E. and A.K. Website: http://english.anisys.ioz.ac.cn/groups/leifumin/introduction/

Author contributions: F.L., Y.Q., P.A., J.F., P.G.P.E and A.K. designed the joint international research project; F.L., R.Z. and G.S conceived the idea for this study; R.Z., G.S. and L.D. collected samples, and R.Z. carried out the lab work; G.S. and R.Z. performed the data analyses, developed the hypotheses and wrote the first draft; Y.Q., A.K., P.A., P.G.P.E., D.L., Z.W. and J.F. discussed results and composed the discussion section of the study. All authors assisted in the interpretation of the results and commented on the manuscript.

Editor: Aristeidis Parmakelis

© 2016 John Wiley & Sons Ltd